HHS Public Access

Author manuscript

Sleep. Author manuscript; available in PMC 2025 August 31.

Published in final edited form as:

Sleep. 2026 February 10; 49(2): . doi:10.1093/sleep/zsaf213.

Unravelling Sleep Apnea Dynamics: Quantifying Loop Gain using Dynamical Modelling of Ventilatory Control

Thijs Nassi[1,2], **Yalda Amidi**[1], **Eline Oppersma**[2], **Dirk W Donker**[2,3], **Nancy S Redeker**[4], **M Brandon Westover**[*,1], **Robert J Thomas**[*,1]

[1]Beth Israel Deaconess Medical Centre, Harvard Medical School, Boston, MA, United States

[2]Cardiovascular and Respiratory Physiology, TechMed Centre, University of Twente, Enschede, The Netherlands

[3]Department of Intensive Care, University Medical Centre Utrecht, Utrecht, The Netherlands

[4]Yale University School of Nursing, New Haven, CT, United States

Abstract

Study Objectives: Loop gain (LG) is a critical parameter for assessing ventilatory control stability in sleep apnea, with implications for personalized treatment. Existing LG estimation methods are hindered by complex processing and specialized equipment, limiting clinical applicability. This study aims to develop an automated method to quantify LG from respiratory inductance plethysmography (RIP) signals to enhance precision management of sleep apnea.

Methods: Polysomnography data from Massachusetts General Hospital, high-altitude studies at Beth Israel Deaconess Medical Centre, and heart failure patients were analysed. Cases included an apnea-hypopnea index >15 and ≥4 hours of recorded sleep. RIP signals were filtered, normalized, and segmented into 8-minute windows. LG estimation employed an augmented Mackey-Glass equation and an expectation-maximization algorithm. Simulation experiments on synthetic breathing data with known parameter values quantified the accuracy of our parameter estimates.

Results: Data from 465 patients were analysed, including 400 patients from the Massachusetts General Hospital dataset and 65 heart failure patients. The method accurately estimated LG across diverse apnea phenotypes. Patients with a higher central apnea index, high self-similarity or heart failure exhibited significantly higher median LG values (0.19, 0.27 and 0.41 respectively) compared to those with obstructive apnea (median LG = 0.11–0.14; $p < 0.001$). In addition, LG was significantly elevated during non-rapid eye movement sleep and at higher altitudes.

Conclusions: The automated LG estimation method developed in this study provides a scalable, non-invasive tool for endotyping in sleep apnea. By accurately modelling patient-specific ventilatory control, this approach supports personalized management strategies in apnea and broader clinical contexts.

Corresponding Author: M. Brandon Westover, M.D. Ph.D., Beth Israel Deaconess Medical Centre, 330 Brookline Avenue, Boston, MA 02215. mwestove@bidmc.harvard.edu.

*Co-senior authors.

Non-Financial Disclosures: None.

Keywords

Sleep Apnea; Loop Gain; Respiratory Control; Mathematical Modelling; Personalized Medicine

INTRODUCTION

Sleep apnea is a prevalent disorder affecting millions globally, with profound implications for cardiovascular health, cognitive function, and overall quality of life [1–3]. Accurate identification of apnea phenotypes, such as obstructive sleep apnea (OSA) and central sleep apnea (CSA) is critical for effective treatment [4,5]. The need for precise assessment of polysomnography (PSG) and home sleep apnea testing data is essential for both diagnosis and personalization of treatment.

Ventilatory control, which is influenced by factors like chemoreflexes, lung mechanics, and arousal thresholds, determines how the body responds to changes in oxygen and carbon dioxide levels, and plays a crucial role in the severity of apnea [6–8]. A key measure of this control is ventilatory loop gain (LG), which indicates the sensitivity of the respiratory system to these changes. A high loop gain (HLG) signifies a more reactive system, potentially leading to breathing instability. In OSA, HLG can exacerbate respiratory instability and complicate interventions [9]. In CSA and Hunter-Cheyne-Stokes respiration (HCSR), increased chemosensitivity (higher controller gain) combined with delayed responses can hinder the body's ability to stabilize breathing, thereby prolonging episodes of unstable breathing and apnea [10].

Recognizing the unique role of LG in apnea subtypes is essential for tailored interventions. For example, OSA patients with average LG should be generally expected respond to continuous positive airway pressure (CPAP) [11], whereas HLG patients may require additional therapy such as O_2, CO_2 therapy, acetazolamide, zonisamide or sulthiame [12–17]. LG assessment aids in the optimization of treatment based on a patient's breathing stability, a decision-support tool.

Despite the availability of several methods for estimating LG in apnea patients, including the use of hypoxic-hypercapnic gas [6,18–21], breath-holding techniques [22–24], mechanical ventilation [25–27], cardiopulmonary coupling [28,29], and mathematical modelling of breathing dynamics [30–32], practical challenges such as manual data annotation and the need for specialized equipment have limited their clinical use. To overcome these barriers, we recently developed an automated algorithm that detects HLG by analysing self-similarity (SS) in the envelope morphology of abdominal respiratory inductance plethysmography (RIP) signals, thereby eliminating the need for manual processing [33,34].

SS quantifies the degree to which the respiratory signal exhibits metronomic repeating, oscillatory patterns. High SS indicates that the breathing pattern is consistently symmetrically oscillatory—a hallmark of increased ventilatory instability and elevated LG. In our approach, the SS metric serves as an indirect marker of LG, indicating expressed HLG rather than the entire spectrum of LG intensities or the physiological interplay of its underlying parameters.

In this study, we present a model-based framework for automated LG assessment based on RIP signals. Our approach uses modified Mackey-Glass equations to model ventilatory control as a closed-loop system, enabling estimation of key parameters including gain and delay in the time domain. By providing a practical method to quantify ventilatory control stability, this work aims to support more targeted treatment selection in sleep apnea and related respiratory disorders.

METHODS

Dataset

The primary data used in this work were selected from an archive containing clinical PSGs from the Massachusetts General Hospital (MGH) sleep laboratory between 2008 and 2022. The MGH and the Beth Israel Deaconess Medical Centre (BIDMC) Institutional Review Boards approved the retrospective analysis of clinically acquired PSG data with waiver of informed consent (protocol #s: MGH: 2013P001024, BIDMC: 2016P000058). The MGH sleep centre is an American Academy of Sleep Medicine (AASM) accredited sleep centre that scores obstructive and central apnea, and hypopnea's using the 4% desaturation rule. Hypopneas meeting the 3% desaturation or arousal criterion were automatically added using a previously developed respiratory event detector [35]. A secondary dataset with heart failure (HF) patients was used to study the known association between HLG and this specific population [36,37]. Thirdly, PSG studies from BIDMC recorded four incremental altitudes were included to show the relationship between LG and high-altitude breathing.

Patient selection based on ventilatory control profile

From all MGH recordings with an apnea–hypopnea index (AHI) >15 (moderate sleep apnea) and ≥4 hours of sleep, we defined four ventilatory control subgroups:

1. "REM OSA": >10% rapid eye movement (REM) sleep and a REM AHI being at least three times higher than the AHI during non-rapid eye movement (NREM).
2. "NREM OSA": >10% REM sleep and a NREM AHI at least double the REM AHI.
3. "High CAI": central apnea index (CAI) >5 with CAI exceeding the obstructive apnea index (OAI).
4. "SS OSA": CAI <5 and >25% of sleep exhibiting high SS.

Additionally, a "SS range" group was selected to encompass the full spectrum of SS levels, where higher SS values are associated with more pronounced oscillatory breathing patterns and thus a higher expressed HLG. One hundred recordings were randomly sampled per subgroup. In the secondary dataset, all patients with AHI >10 and left ventricular ejection fraction <50% comprised the "Heart Failure" group.

Preprocessing

Abdominal RIP signals were extracted with a sampling frequency of 200Hz or 512Hz using the Natus system; in our data, thoracic effort signals were noisier. After applying a notch filter of 60Hz (to remove power line noise) and a lowpass filter of 10Hz to

reduce non-physiological noise, all recordings were resampled to 10Hz. Next, recordings were normalized using the mean and standard deviation of the 5^{th}-95^{th} percentile clipped signal. Ventilatory envelopes were computed by connecting inspiratory and expiratory amplitude peaks, from which reductions of 30% and 90% for a duration >10 seconds were associated with hypopnea and apnea, respectively. A surrogate for ventilation was derived continuously from RIP signals and analyzed in the time domain. Sharp increases in ventilation—defined as a rapid rise where the smoothed difference, calculated using a 10-second rolling maximum over a 3-second evaluation window, exceeds a threshold of 0.5—were flagged as potential arousal locations, typically occurring at the end of respiratory events. This approach effectively isolates significant ventilatory spikes indicative of arousal while minimizing the impact of minor fluctuations.

Segmentation

Characterizing ventilatory control overnight is difficult as its dynamics typically fluctuate [38]. To assess the fragmented nature of expressed HLG in patients, we employed our published SS algorithm in combination with a change-point detector [39] to approximate the most common duration of expressed HLG in breathing. We then analyzed the “SS range” group by constructing a histogram of the lengths of high SS segments and determined that the median duration was 8 minutes. This window length represents a balancing act: a window that is too short may fail to capture the full dynamics of ventilatory control, whereas a window that is too long may average over important temporal variations. Therefore, we selected an 8-minute window to reliably capture episodes of expressed HLG while preserving the inherent fluctuations in ventilatory control.

Modelling and estimation of ventilatory control

For each 8-minute segment of breathing data we modelled the local dynamics of ventilatory control.

The Mackey-Glass equations serve as the cornerstone of our methodology:

$$\dot{x}(t) = L - v_d(t-\tau)x(t), \quad where \;\; v_d(t) = \frac{V_{max} \cdot x^{\gamma}(t)}{1 + x^{\gamma}(t)}$$

which states that the rate of change of the arterial CO_2 concentration, x, is the CO_2 production rate, L, minus the ventilation rate a brief time τ in the past, $v_d(t-\tau)$, times the current CO_2 concentration. Here, τ is the delay between plant (the lungs) and the controller (the brainstem).

In our model, the “plant” refers to the physical components (such as the lungs and associated structures) responsible for gas exchange, and its gain—commonly termed Plant Gain (PG)—describes how changes in ventilation affect arterial CO_2 levels. The “controller” represents the chemoreflex mechanism, primarily located in the brainstem, which responds to deviations in CO_2 levels; its sensitivity is captured by the parameter $\boldsymbol{\gamma}$, referred to as Controller Gain (CG). Although our closed-loop system identification does not directly measure CO_2 and therefore does not allow for complete separation of PG and CG, the

parameter γ predominantly reflects the responsiveness of the controller. The overall Loop Gain (LG) integrates these components by quantifying the system's feedback sensitivity, defined as the ratio of the ventilatory response to the magnitude of the disturbance. In essence, while PG (which is also influenced by parameters such as V_{max}) and CG represent the individual contributions of the respiratory system and its regulatory feedback, LG reflects their combined effect in determining whether the system maintains stability or exhibits oscillatory behavior.

The ventilation rate $v_d(t)$ in turn is modeled as a sigmoid curve with two parameters: V_{max}, the maximum ventilation rate, and γ the controller gain (steepness of the sigmoid curve), such that ventilation increases with higher levels of CO_2. Building upon Equation 1, we introduce a parameter for breathing disturbance $v_d(t)$, corresponding to the reduction in ventilation during apneas or hypopneas, and a parameter for arousals (v_{ar}), which cause transient increases in ventilation. With these modifications, we rewrite the original Mackey-Glass equations as:

$$\dot{x}(t) = L - v_o(t-\tau)x(t), \quad \text{where} \quad v_o(t) = v_d(t)\,\alpha U(t) + v_{ar}(t)$$

In this ventilatory control model we assume a constant CO_2 production rate (L = 0.05) and we derived $U(t)$ and $v_{ar}(t)$ a priori from the surrogate ventilation traces, where $U(t)$ is based on the automatically scored respiratory events.

To recover the unobserved physiological state (i.e., arterial CO_2 concentration), from observed ventilation data, we employed a recursive Bayesian filter based on a Gaussian approximation. At each time step, the filter simulated the system's state evolution using the Mackey-Glass equations, generating a prior (one-step prediction) for the current state. This prior was then updated by incorporating the latest observation through a closed-form update rule derived from the first and second derivatives of the log-likelihood function. The recursive nature of this approach allowed for real-time tracking of state dynamics, while a fixed-interval smoother was subsequently applied to refine these estimates using the entire observation window.

All other parameters, i.e., γ, τ, α, V_{max}, and the height of each individual arousal, are treated as hidden parameters to be estimated. To estimate these hidden parameters, we used the expectation-maximation (EM) algorithm [40]. Initially, in the E step, this algorithm estimates the hidden parameters by computing their probability distribution based on the observed ventilation data from patients. Subsequently, in the M step, it refines the model's parameters by maximizing the expected log-likelihood computed in the E step. By iteratively switching between these steps, the EM algorithm optimizes the model's parameters, by reducing the root mean square error (RMSE) between the modelled v_o and observed ventilation derived from the RIP signals.

Given the estimated parameters, we compute LG by analysing the system's response to disturbances and subsequent recovery. Specifically, LG is computed as the ratio of the change in ventilation immediately following the end of an apnea or hypopnea (the

"disturbance"), (ΔV_R), to the change in ventilation induced by the disturbance (ΔV_D). Here, ΔV_R is the absolute difference between the steady-state ventilation ΔV_{SS} and the ventilation after removing the disturbance, while ΔV_D represents the absolute difference between ΔV_{SS} and the ventilation during the disturbance. We define the steady-state ventilation as the average ventilation over each 8-minute segment, excluding periods of respiratory events and arousals. This average is assumed to approximate eupneic breathing and serves as the reference point for quantifying the ventilation disturbances and responses in the calculation of LG. This ratio, $LG = \Delta V_R / \Delta V_D$, quantifies the system's feedback sensitivity, determining whether the system maintains stability or exhibits oscillatory behaviour. For additional mathematical details, including the derivation of the Mackey-Glass equations, the development of the recursive Bayesian filter and fixed-interval smoother, and the physiologically informed constraints used in parameter estimation, please refer to the Supplemental Material.

Simulation and validation of the LG estimator

Although no direct ground truth for loop gain exists in clinical data, we addressed this through simulation studies. By generating synthetic breathing data with known parameter values (varying γ from 0.1–2.0 and τ from 5–50 seconds), we quantified the accuracy of our parameter estimation. These simulations demonstrated that our method reliably recovers the true values (e.g., RMSE for τ consistently <2 s and high correlation coefficients for γ), thereby substantiating that our system accurately models ventilatory control. Boxplots displayed parameter distributions for REM OSA, NREM OSA, SS OSA, and high CAI groups, with T-tests comparing REM OSA to other subgroups for LG and γ. A scatterplot with a 2nd order polynomial fit (95% confidence interval with 10,000 bootstraps) of the "SS range" group, including its r^2 value and 5th-95th percentile range. Boxplots were created showing the distribution of the estimated LG within NREM vs. REM within the "SS range" group. For the altitude data, histograms of the estimated LG distribution were created. Unpredictable LG segments (fewer than 5 apneas/hypopneas in 8-minute windows) were excluded. The 95th percentile LG value per patient highlighted LG trends across increasing altitudes, minimizing regular breathing effects and outliers.

Predicting CPAP failure

We selected recordings from patients with a baseline AHI >10 and at least 4 hours of sleep. During the CPAP titration phase, patients were classified based on their AHI and CAI: successes were defined as those with an AHI <10 and CAI <5, whereas failures were defined as those with an AHI ≥30 or CAI ≥10 despite CPAP. Two hundred patients were sampled from each group. Predictive performance was then evaluated by computing receiver operating characteristic (ROC), precision-recall (PR), and calibration curves for three feature sets: CAI alone, a combination of the median and interquartile range of LG estimates, and the combined CAI and LG features.

RESULTS

Dataset

Data from MGH and BIDMC are summarized in Table 1. The “Heart Failure” group included 65 patients. Altitude data from 8 patients with recordings at sea level, 5, 8, and 13 thousand feet were analysed. High SS chunks (expressed HLG) in the “SS range” group, summarized in a histogram (Figure S2), typically lasted 4–10 minutes, with a median duration of approximately 8 minutes.

Simulation experiments

Simulation experiments demonstrated that the LG estimator reliably recovers the true parameter values. When the EM algorithm was initialized with the true values, the estimated parameters closely matched the simulation settings (Figure S3, grey line). To evaluate performance in non-simulated clinical scenarios, we assessed two different initialization approaches for the EM algorithm: (i) fixed parameter initialization, and (ii) a “warm start” approach that runs 5 parallel initializations and selects the best result. Both methods yielded similar parameter recovery across three simulation experiments. Specifically, strong positive correlations were observed between the median estimated and simulated values for γ, although higher γ values tended to be slightly underestimated, and median τ estimates were nearly perfect across all simulations. Given that the fixed parameter initialization was approximately 5-fold faster than the warm start approach, we opted to use the fixed parameter initialization for the subsequent analysis of clinical data. Contour plots of the RMSE for simulated versus estimated values of γ and τ (Figure S4) further demonstrated that lower γ estimates were associated with higher accuracy, while RMSE for τ consistently remained below 2 seconds over its physiological range. Our computational performance analysis indicates that processing a single night’s recording takes approximately 5 minutes on a standard computer, with the entire procedure being fully automated and requiring no manual intervention.

Modelling ventilatory control

Figure 1 depicts six 8-minute breathing segments from patients suffering from various apnea phenotypes. From top to bottom, the figures show two segments of a patient exhibiting HCSR with overt centrally driven events and HLG; 2 segments of patient with predominantly obstructive apneas with respective low and high estimated LG; 2 segments with mostly hypopneas with a corresponding low and high estimated LG. Corresponding LG values were found after estimating the underlying hidden dynamics that resulted in the best fit with the patient’s breathing data, i.e., the parameter combination of γ, τ, α, and V_{max} that minimized the RMSE between the overserved and modelled ventilation. Note how the modelled v_d closely resembles the patient’s ventilation trend and v_{ar}, matches the peak ventilation amplitude following respiratory events. Figure 2 shows a full-night RIP recording of a patient with HCSR including the varying LG estimations for all 8-minute segments of consecutive NREM or REM sleep (without intermittent wake). Note that the respiratory events and high SS breathing oscillations are automatically labelled by our SS detector.

LG across patient ventilatory control profiles

Boxplots in Figure 3 show the distribution of the estimated LG, γ, and τ values across patient subgroups. Patients from the “REM OSA” group show the lowest median LG. Relative to this group, all other groups showed higher median LG and γ values with strong significance ($p<0.001$). Notably, LG and γ exhibited parallel trends and strong correspondence, with both metrics increasing progressively across the “high CAI,” “SS OSA,” and “Heart Failure” ventilatory control profile groups. A median τ of 26 seconds was found for the “Heart Failure” patients, whereas median values closer to 20 seconds were found for the other apnea subgroups. Swimmer plots and bar graphs of the LG estimations from 20 nights of each of the ventilatory control profiles of the MGH dataset are visualized in Figure 4. Compared to the “REM OSA” group, the proportion of HLG among the other ventilatory control profiles is markedly increased.

SS vs LG

To characterize the relationship between the estimated LG and expressed LG, as measured through self-similarity (SS), Figure 5 shows a scatterplot including the 5^{th}-95^{th} percentile range. A 2^{nd} order polynomial fit to the data has an r^2 value of 0.75, indicating a strong monotonic relationship. The LG distribution across all NREM segments showed a higher median compared to during REM sleep, shown in Figure 6.

Altitude vs LG

Estimations from our LG model for 8 patient recordings at varying altitudes are shown in Figure 7. The upper section displays normalized histograms of LG distributions at sea level, 5000 ft, 8000 ft, and 13,000 ft. The bottom left graph shows an increasing trend in the 95^{th} percentile LG (triangles), while the bottom right graph depicts the percentage of high SS (expressed HLG) breathing oscillations. Both indicate higher mean and median LG at elevated altitudes compared to sea level. Interestingly, for some patients (e.g., 2 and 5), HLG levels were higher at 5000/8000 ft than at 13,000 ft.

Predicting CPAP failure

The CAI model achieved a ROC AUC of 0.68 and a PR AUC of 0.66, while the LG model yielded ROC and PR AUCs of 0.65 and 0.63, respectively, both indicating a similar ability in predicting patients with poor CPAP-related outcomes. Notably, the combined CAI and LG model significantly improved performance with a ROC AUC of 0.78 and a PR AUC of 0.71 (see Figure 8), demonstrating that integrating these features enhances the predictive capability for CPAP failure compared to using either feature alone.

DISCUSSION

This study presents a novel method for estimating LG and its ventilatory control parameters using RIP signals. By applying modified Mackey-Glass equations to overnight breathing data, the approach offers a practical, equipment-free assessment of ventilatory stability. Our results indicate its potential to differentiate LG patterns in diverse sleep-disordered breathing populations. This capability, using routine clinical signals, could guide treatment selection

and improve outcomes, especially in cases where ventilatory control instability exacerbates sleep apnea severity.

LG measurements offer valuable potential for clinical decision-making in sleep apnea treatment. HLG can predict CPAP intolerance, inadequate treatment response, and persistent residual apnea, allowing clinicians to stratify patients by risk and optimize therapy selection [34,41–43]. When considering alternative treatments such as oral appliances or hypoglossal nerve stimulation, LG assessment can identify patients who may require additional interventions targeting ventilatory control stability (e.g., acetazolamide or supplemental oxygen) [12–16]. Our automated approach provides unique advantages by enabling continuous monitoring of LG dynamics across multiple time scales. This allows quantification of how LG varies with body position [44,45], time of night [46], night-to-night if multi-night data is available, sleep stage, and overall sleep quality at an individual patient level. The method can also track treatment effectiveness over time. While self-similarity mapping provides complementary information about breathing patterns, our LG measurements can possibly stand alone as an independent metric for assessing ventilatory control stability.

Our findings reveal significant differences in LG across patient groups. Patients with high CAI, elevated SS scores, or heart failure had the highest median LG (0.41) and significantly higher controller gain than the REM-dominant OSA group, emphasizing the prominent role of ventilatory control instability in these populations. Heart failure patients also exhibited the highest median chemosensitivity delay, reflecting chronic respiratory control alterations.

In contrast, the REM-dominant OSA group exhibited a low median LG of 0.11 with relatively small variability. Nearly no LG values greater than 0.4 were estimated by the EM algorithm for patients with this ventilatory control profile. This finding aligns with our understanding that classic OSA in this group involves stable mechanical obstruction with less influence from ventilatory control instability.

The NREM-dominant OSA group, likely representing a more heterogeneous mixture of obstructive and central pathologies, showed a significant increase in median LG and higher variability compared to the REM-dominant group. This suggests a complex interplay between physical obstruction and ventilatory control mechanisms, highlighting the necessity for personalized treatment strategies in this subgroup.

The relationship between altitude and LG was explored using data from healthy patients recorded at various elevations. The results indicated that overnight breathing at sea level is associated with a lower LG compared to higher altitudes. Both average LG and the percentage of sleep with high SS breathing oscillations increased with altitude, consistent with known physiological responses to hypoxia, which include increased chemosensitivity and changes in arousal thresholds. While it is known that the low oxygen at altitude induces sensitization of the hypoxic ventilatory response, acclimatization was also observed in multiple subjects.

The gradual increase in average LG across categories, despite remaining low (~0.5), underscores the multifactorial nature of ventilatory control instability. While stable breathing

periods were excluded, unstable periods vary in morphology and drivers even within the same individual. In subgroups like NREM-dominant OSA, heart failure, and high-altitude apnea, factors such as arousals and airway vulnerabilities influence sleep apnea pathophysiology independently of LG. Periods of SS almost have high loop gain. Similarly, SS varies dynamically and rarely reaches 100% expression across a full sleep period, consistent with the observed median segment duration of 8 minutes. These findings emphasize the complex factors influencing ventilatory control and their importance in personalized sleep apnea management.

Importantly, our analysis of CPAP failure prediction further underscores the clinical utility of our integrated approach. The LG and CAI models alone achieved similar discrimination in identifying patients at risk for poor CPAP outcomes; however, combining CAI and LG features significantly improved predictive accuracy, yielding a ROC AUC of 0.78 and a PR AUC of 0.71 (see Figure 8). These findings indicate that integrating conventional respiratory indices with dynamic ventilatory control measures more effectively captures the complex pathophysiology of sleep-disordered breathing, thereby enhancing patient stratification and facilitating more personalized therapeutic strategies. These results are consistent with our earlier work [34]. Loop gain assessments are probably going to be most useful clinically when the traditional CAI is relatively low.

Recent studies emphasize central mechanisms in OSA, suggesting drive-dependent OSA, characterized by declining ventilatory drive, accounts for many cases [47]. This has significant implications for apnea therapy, highlighting the need to address and stabilize neural ventilatory drive by targeting treatments that either elevate or prevent its decline in addition to mechanical airway patency. Understanding and detecting LG can thus play a critical role in diagnosing and treating drive-dependent OSA.

To promote patient-level endotype targeted apnea therapy, the proposed method offers a clinically applicable approach to study patient-specific ventilatory LG. While measuring LG using mechanical ventilation has been established for several decades [25,26,48], this method requires dedicated equipment which is typically not available during routing sleep studies. The more recent PUP method that can analyse LG from standard PSG signals made an important step towards the clinical implementation of LG estimation [32,49], However, while the PUP method relies on standard PSG scoring—including exhaustive manual or automated labeling of respiratory events—the current approach only requires RIP, sleep staging and automated arousal detection, substantially reducing the annotation burden (including the need to check event-scoring accuracy) while achieving comparable outcomes. Moreover, by leveraging a RIP signal, our method provides a robust, continuous surrogate of ventilatory drive with fewer artifacts than nasal pressure/flow signals, and by analyzing ventilation in the time domain rather than on a breath-by-breath basis, it captures both steady-state and transient dynamics within a unified model. These refinements facilitate a more streamlined, patient-specific estimation of ventilatory loop gain, thereby enhancing the clinical applicability of targeted apnea therapy. Cardiopulmonary coupling can identify HLG through detection of narrow-band coupling, which reflects SS patterns in physiological rhythms. However, this approach necessitates 15–17 uninterrupted minutes of consistent cardiopulmonary oscillations to be effective [28,29], making it less sensitive to

short bursts of periodic breathing. Limitations of our previous work using SS in RIP data include the method's high sensitivity in detecting SS oscillations [34], which sometimes leads to the inclusion of noise, especially at lower SS scores. The proposed approach rivals the accuracy of current LG estimation standards while enabling broader implementation by relying solely on RIP signals, eliminating the need for event labelling. This innovation offers opportunities for scalable and precise LG estimation, crucial for personalized OSA therapy. The method could also be adapted for home sleep apnea testing using respiratory effort tracking. However, further validation is needed to extend LG measurements to non-standard signals such as oximetry, jaw movements, or pulse photoplethysmography.

Limitations

Although we leverage the RIP envelope as a continuous proxy for ventilation, RIP amplitude does not directly equate to airflow. During obstructive apneas, thoraco-abdominal movements may persist despite upper-airway closure, producing residual RIP excursions that overestimate ventilation and thus underestimate CO_2 accumulation. This can bias our loop-gain estimates upward; future work should consider direct airflow measurements or correction factors during confirmed obstructive events.

Quantifying LG parameters across an entire overnight study requires caution. Even in patients with severe HLG, some segments will show apneas amplified by an underlying increased gain, whereas other parts of the recording, e.g., during REM, can display regular breathing or classic OSA with a normal LG. Stable breathing periods without events can lower whole-night LG averages. Our empirical approach using 8-minute windows provided robust estimates, but LG's variability highlights the need for careful consideration of window size and estimation resolution. Future work should refine and validate these methods across diverse patient populations.

Occasionally, the model is inaccurate in predicting HLG for individual segments, particularly exhibiting a tendency to underestimate the controller gain parameter, γ. This underestimation was also observed in our simulation experiments, suggesting a bias in the model's performance for higher LG values. Nevertheless, this limitation presents limited practical problems when assessing a patient's overall LG across an entire recording. The aggregation of segmental estimates mitigates the impact of occasional underestimation, providing a reliable overall assessment of a patient's ventilatory control stability, as demonstrated in Figure 3.

A limitation of our study is that we did not directly compare our loop gain estimates to those obtained from gold-standard methods such as CPAP dial-down. Although our method provides quantitative LG estimates from observational data, future studies should validate these estimates against established techniques. Until such comparisons are available, our LG values should be regarded as guidelines rather than absolute measurements. Furthermore, our results, particularly the ability to predict CPAP adherence, underscore the clinical relevance and interpretability of our approach.

The accuracy of this method relies on high-quality respiratory signals. Physicians should interpret LG estimates as guidelines, not absolute values, to identify patients at higher risk

of ventilatory instability. These insights could inform therapies targeting ventilatory control stability, such as strengthening respiratory drive [17,50,51] alongside traditional treatments for mechanical airway obstruction, potentially enhancing treatment outcomes through a personalized approach.

Conclusions

This study advances the understanding of ventilatory control dynamics in sleep apnea by providing a novel, automated method to estimate LG and its stability parameters. Our findings underscore the importance of personalized approaches to apnea management, considering the complex interplay between mechanical and neural factors in respiratory control. Further research and clinical validation are essential to fully integrate these methods into routine practice, ultimately improving patient outcomes through tailored therapy strategies.

Supplementary Material

Refer to Web version on PubMed Central for supplementary material.

Sources of Support:

This work was supported by grants from the NIH (R01NS102190, R01NS102574, R01NS107291, RF1AG064312, RF1NS120947, R01AG073410, R01HL161253, R01NS126282, R01AG073598, R01NR08022), and NSF (2014431).

Financial Disclosures:

Dr. Westover is a co-founder, scientific advisor, consultant to, and holds personal equity interest in Beacon Biosignals. Dr. Thomas holds a licensed patent to MyCardio, LLC, for the use of ECG/PPG spectrogram technology to assess sleep quality, sleep apnea, and sleep apnea endotypes; has submitted a patent for Enhanced Expiratory Rebreathing Space (EERS), a CO_2-regulating treatment for central sleep apnea; and serves as a consultant for Guidepoint and GLG Councils. Drs. Thomas, Oppersma, and Westover, along with Thijs Nassi, have jointly submitted a patent for the detection and quantification of respiratory self-similarity.

DATA AVAILABILITY STATEMENT

The data underlying this article will be shared upon publication, at https://bdsp.io/ and can be accessed per request to the corresponding author.

REFERENCES

1. Lajoie AC, Lafontaine AL, Kimoff RJ, Kaminska M. Obstructive Sleep Apnea in Neurodegenerative Disorders: Current Evidence in Support of Benefit from Sleep Apnea Treatment. J Clin Med. 2020; 9 (2).
2. Zhao X, Li X, Xu H, et al. Relationships between cardiometabolic disorders and obstructive sleep apnea: Implications for cardiovascular disease risk. J Clin Hypertens. 2019; 21 (2): 280–290.
3. Bjornsdottir E, Keenan BT, Eysteinsdottir B, et al. Quality of life among untreated sleep apnea patients compared to the general population and changes after treatment with positive airway pressure. Journal of sleep research. 2015; 24 (3).
4. Ramirez J-M, Alfredo J. Garcia I, Anderson TM, et al. Central and Peripheral factors contributing to Obstructive Sleep Apneas. Respiratory physiology & neurobiology. 2013; 189 (2).
5. Zinchuk A, Gentry M, Concato J, Yaggi K. Phenotypes in obstructive sleep apnea: a definition, examples and evolution of approaches. Sleep medicine reviews. 2017; 35.

6. Loewen A, Ostrowski M, Laprairie J, et al. Determinants of ventilatory instability in obstructive sleep apnea: inherent or acquired? Sleep. 2009; 32 (10): 1355–1365. [PubMed: 19848364]
7. Wellman A, Jordan AS, Malhotra A, et al. Ventilatory Control and Airway Anatomy in Obstructive Sleep Apnea. American journal of respiratory and critical care medicine. 2004; 170 (11).
8. Lee JJ, Sundar KM. Evaluation and Management of Adults with Obstructive Sleep Apnea Syndrome. Lung. 2021; 199 (2): 87–101. [PubMed: 33713177]
9. Deacon NL, Catcheside PG. The role of high loop gain induced by intermittent hypoxia in the pathophysiology of obstructive sleep apnoea. Sleep Med Rev. 2015; 22: 3–14. [PubMed: 25454671]
10. Orr JE, Malhotra A, Sands SA. Pathogenesis of Central and Complex Sleep Apnoea. Respirology. 2017; 22 (1).
11. Stanchina M, Robinson K, Corrao W, Donat W, Sands S, Malhotra A. Clinical Use of Loop Gain Measures to Determine Continuous Positive Airway Pressure Efficacy in Patients with Complex Sleep Apnea. A Pilot Study. Annals of the American Thoracic Society. 2015; 12 (9).
12. Sands SA, Edwards BA, Terrill PI, et al. Identifying obstructive sleep apnoea patients responsive to supplemental oxygen therapy. Eur Respir J. 2018; 52 (3).
13. Mulchrone A, Shokoueinejad M, Webster J. A review of preventing central sleep apnea by inspired CO2. Physiol Meas. 2016; 37 (5): R36–45. [PubMed: 27093535]
14. Edwards BA, Sands SA, Eckert DJ, et al. Acetazolamide improves loop gain but not the other physiological traits causing obstructive sleep apnoea. J Physiol. 2012; 590 (5): 1199–1211. [PubMed: 22219335]
15. Eskandari D, Zou D, Karimi M, Stenlof K, Grote L, Hedner J. Zonisamide reduces obstructive sleep apnoea: a randomised placebo-controlled study. Eur Respir J. 2014; 44 (1): 140–149. [PubMed: 24627538]
16. Schmickl CN, Landry S, Orr JE, et al. Effects of acetazolamide on control of breathing in sleep apnea patients: Mechanistic insights using meta-analyses and physiological model simulations. Physiol Rep. 2021; 9 (20): e15071. [PubMed: 34699135]
17. Hedner J, Stenlof K, Zou D, et al. A Randomized Controlled Clinical Trial Exploring Safety and Tolerability of Sulthiame in Sleep Apnea. Am J Respir Crit Care Med. 2022; 205 (12): 1461–1469. [PubMed: 35202553]
18. McClean PA, Phillipson EA, Martinez D, Zamel N. Single breath of CO2 as a clinical test of the peripheral chemoreflex. J Appl Physiol (1985). 1988; 64 (1): 84–89. [PubMed: 3128530]
19. Ghazanshahi SD, Khoo MC. Estimation of chemoreflex loop gain using pseudorandom binary CO2 stimulation. IEEE Trans Biomed Eng. 1997; 44 (5): 357–366. [PubMed: 9125820]
20. Hudgel DW, Gordon EA, Thanakitcharu S, Bruce EN. Instability of ventilatory control in patients with obstructive sleep apnea. Am J Respir Crit Care Med. 1998; 158 (4): 1142–1149. [PubMed: 9769273]
21. Younes M, Ostrowski M, Atkar R, Laprairie J, Siemens A, Hanly P. Mechanisms of breathing instability in patients with obstructive sleep apnea. J Appl Physiol (1985). 2007; 103 (6): 1929–1941. [PubMed: 17823298]
22. Stanley NN, Cunningham EL, Altose MD, Kelsen SG, Levinson RS, Cherniack NS. Evaluation of breath holding in hypercapnia as a simple clinical test of respiratory chemosensitivity. Thorax. 1975; 30 (3): 337–343. [PubMed: 1145539]
23. Trembach N, Zabolotskikh I. Breath-holding test in evaluation of peripheral chemoreflex sensitivity in healthy subjects. Respir Physiol Neurobiol. 2017; 235: 79–82. [PubMed: 27756650]
24. Messineo L, Taranto-Montemurro L, Azarbarzin A, et al. Breath-holding as a means to estimate the loop gain contribution to obstructive sleep apnoea. J Physiol. 2018; 596 (17): 4043–4056. [PubMed: 29882226]
25. Meza S, Younes M. Ventilatory stability during sleep studied with proportional assist ventilation (PAV). Sleep. 1996; 19 (10 Suppl): S164–166. [PubMed: 9085500]
26. Younes M, Ostrowski M, Thompson W, Leslie C, Shewchuk W. Chemical control stability in patients with obstructive sleep apnea. Am J Respir Crit Care Med. 2001; 163 (5): 1181–1190. [PubMed: 11316657]

27. Wellman A, Eckert DJ, Jordan AS, et al. A method for measuring and modeling the physiological traits causing obstructive sleep apnea. J Appl Physiol (1985). 2011; 110 (6): 1627–1637. [PubMed: 21436459]
28. Ramar K, Desrues B, Ramar P, Morgenthaler TI. Analysis of cardiopulmonary coupling to assess adaptive servo-ventilation success in complex sleep apnea management. Sleep Breath. 2013; 17 (2): 861–866. [PubMed: 23117897]
29. Al Ashry HS, Ni Y, Thomas RJ. Cardiopulmonary Sleep Spectrograms Open a Novel Window Into Sleep Biology-Implications for Health and Disease. Front Neurosci. 2021; 15: 755464. [PubMed: 34867165]
30. Terrill PI, Edwards BA, Nemati S, et al. Quantifying the ventilatory control contribution to sleep apnoea using polysomnography. Eur Respir J. 2015; 45 (2): 408–418. [PubMed: 25323235]
31. Nava-Guerra L, Edwards BA, Terrill PI, et al. Quantifying ventilatory control stability from spontaneous sigh responses during sleep: a comparison of two approaches. Physiol Meas. 2018; 39 (11): 114005. [PubMed: 30465721]
32. Finnsson E, Olafsdottir GH, Loftsdottir DL, et al. A scalable method of determining physiological endotypes of sleep apnea from a polysomnographic sleep study. Sleep. 2021; 44 (1).
33. Oppersma E, Ganglberger W, Sun H, Thomas RJ, Westover MB. Algorithm for automatic detection of self-similarity and prediction of residual central respiratory events during continuous positive airway pressure. Sleep. 2021; 44 (4).
34. Nassi TE, Oppersma E, Labarca G, Donker DW, Westover MB, Thomas RJ. Morphological Prediction of CPAP Associated Acute Respiratory Instability. Annals of the American Thoracic Society. 2024.
35. Nassi TE. Algorithms for Automated Scoring of Respiratory Events in Sleep. Enschede, Netherlands, University of Twente; 2021.
36. Redeker NS, Jeon S, Muench U, Campbell D, Walsleben J, Rapoport DM. Insomnia Symptoms and Daytime Function in Stable Heart Failure. Sleep. 2010; 33 (9).
37. Redeker NS, Muench U, Zucker MJ, et al. Sleep Disordered Breathing, Daytime Symptoms, and Functional Performance in Stable Heart Failure. Sleep. 2010; 33 (4).
38. Landry SA, Andara C, Terrill PI, et al. Ventilatory control sensitivity in patients with obstructive sleep apnea is sleep stage dependent. Sleep. 2018; 41 (5).
39. Truong C, Oudre L, Vayatis N. Selective review of offline change point detection methods. Signal Processing. 2020; 167.
40. Do CB, Batzoglou S, Do CB, Batzoglou S. What is the expectation maximization algorithm? Nature Biotechnology. 2008; 26 (8).
41. Mulgrew AT, Lawati NA, Ayas NT, et al. Residual sleep apnea on polysomnography after 3 months of CPAP therapy: clinical implications, predictors and patterns. Sleep Med. 2010; 11 (2): 119–125. [PubMed: 20083429]
42. Denotti AL, Wong KK, Dungan GC, Gilholme JW, Marshall NS, Grunstein RR. Residual sleep-disordered breathing during autotitrating continuous positive airway pressure therapy. Eur Respir J. 2012; 39 (6): 1391–1397. [PubMed: 22075478]
43. Reiter J, Zleik B, Bazalakova M, Mehta P, Thomas RJ. Residual Events during Use of CPAP: Prevalence, Predictors, and Detection Accuracy. J Clin Sleep Med. 2016; 12 (8): 1153–1158. [PubMed: 27166303]
44. Joosten SA, Landry SA, Sands SA, et al. Dynamic loop gain increases upon adopting the supine body position during sleep in patients with obstructive sleep apnoea. Respirology. 2017; 22 (8).
45. Messineo L, Joosten S, Perger E. Mechanisms relating to sleeping position to the endotypes of sleep disordered breathing. Current Opinion in Pulmonary Medicine. 2023; 29 (6).
46. Tkacova R, Niroumand M, Lorenzi-Filho G, Bradley TD. Overnight Shift From Obstructive to Central Apneas in Patients With Heart Failure. Circulation. 2001; 103 (2).
47. Gell LK, Vena D, Alex RM, et al. Neural ventilatory drive decline as a predominant mechanism of obstructive sleep apnoea events. Thorax. 2022; 77 (7): 707–716. [PubMed: 35064045]
48. Dempsey JA. Central sleep apnea: misunderstood and mistreated! F1000Res. 2019; 8.

49. Orr JE, Sands SA, Edwards BA, et al. Measuring Loop Gain via Home Sleep Testing in Patients with Obstructive Sleep Apnea. American Journal of Respiratory and Critical Care Medicine. 2018; 197 (10).

50. Ni YN, Holzer RC, Thomas RJ. Acute and long-term effects of acetazolamide in presumed high loop gain sleep apnea. Sleep Med. 2023; 107: 137–148. [PubMed: 37178545]

51. Quinn T, Thomas RJ, Heckman EJ. Enhanced expiratory rebreathing space for high loop gain sleep apnea treatment. Frontiers in Sleep. 2023; 2.

STATEMENT OF SIGNIFICANCE

This study presents an innovative method for estimating ventilatory control stability using respiratory inductance plethysmography signals, offering a practical, scalable solution for routine clinical use. By enabling detailed characterization of ventilatory control dynamics, the method can differentiate sleep apnea phenotypes and identify patients at elevated risk of ventilatory instability. This has direct clinical implications, such as guiding personalized treatment strategies, predicting continuous positive airway pressure tolerance, and flagging patients for possible adjunctive therapies like oxygen supplementation or carbonic anhydrase inhibitors. Furthermore, the fully automated nature of our approach enables repeated assessments over time, facilitating longitudinal monitoring of treatment efficacy and disease progression. By advancing diagnostic precision and treatment tailoring, this innovation has the potential to improve the management of sleep-disordered breathing and related conditions.

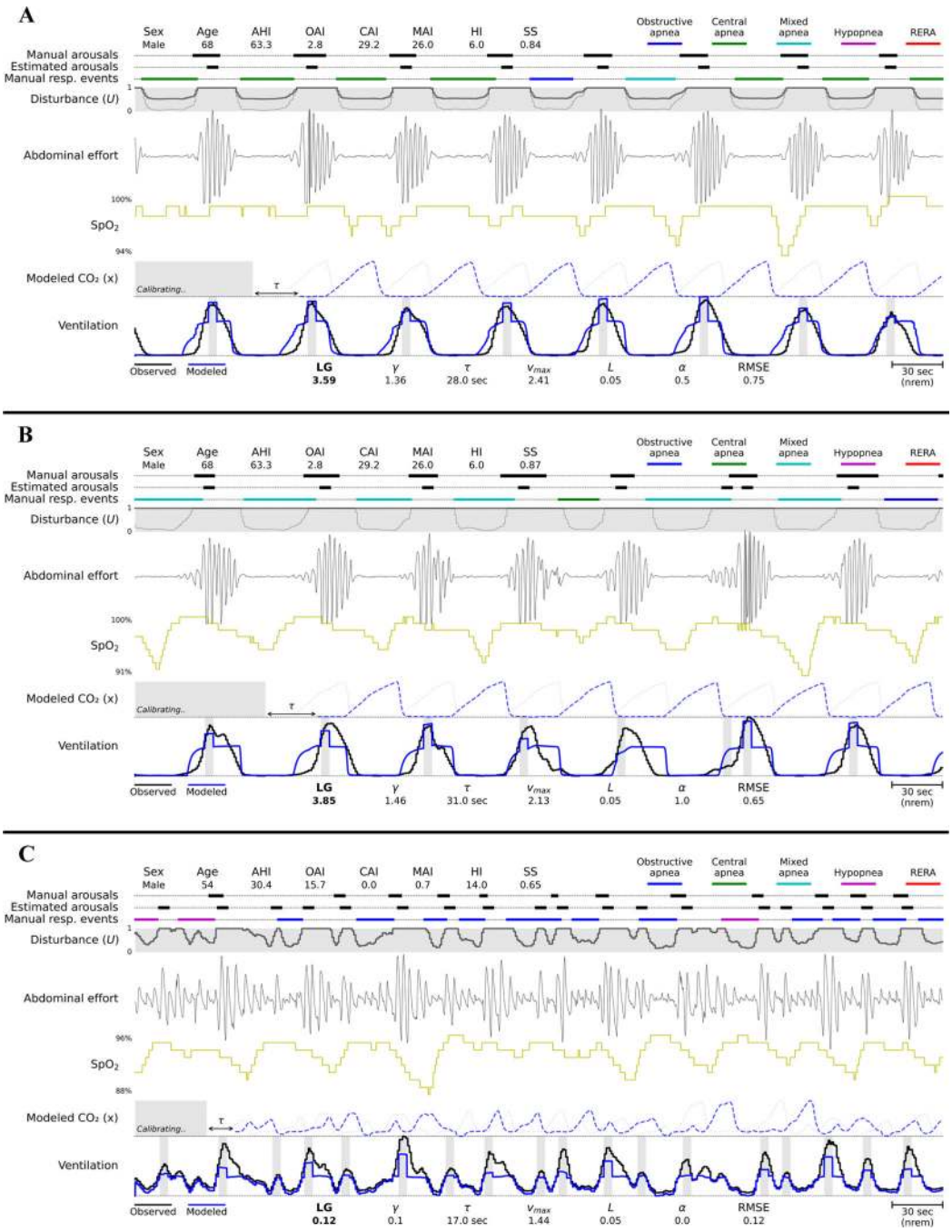

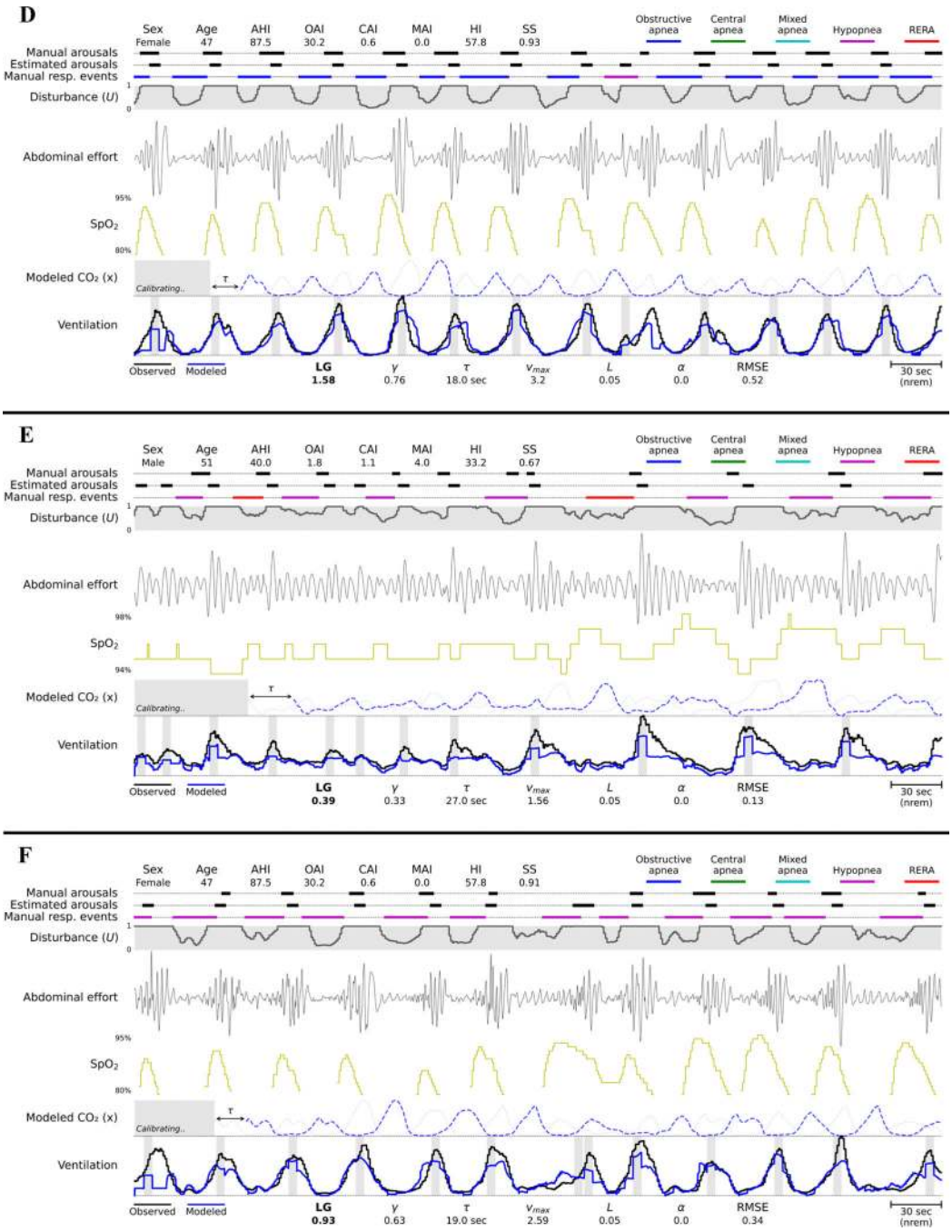

Figure 1:

Six 8-minute examples of apnea patients with varying ventilatory control profiles and their respective estimated stability parameters. a-b: 2 segments of a patient showing Cheyne-Stokes respirations with overt centrally driven events and a high loop gain (LG); c-d: segments of patient with predominantly obstructive apneas with respective low and high LG; e-f: segments with mostly hypopneas with an estimated corresponding low and high LG. Estimated parameters for each segment are displayed at the bottom of each subfigure.

γ=gain, τ=delay, V_{max}=maximum ventilation rate, L= CO_2 production rate, α=disturbance scaling, RMSE=root mean square error between the modelled and the observed ventilation.

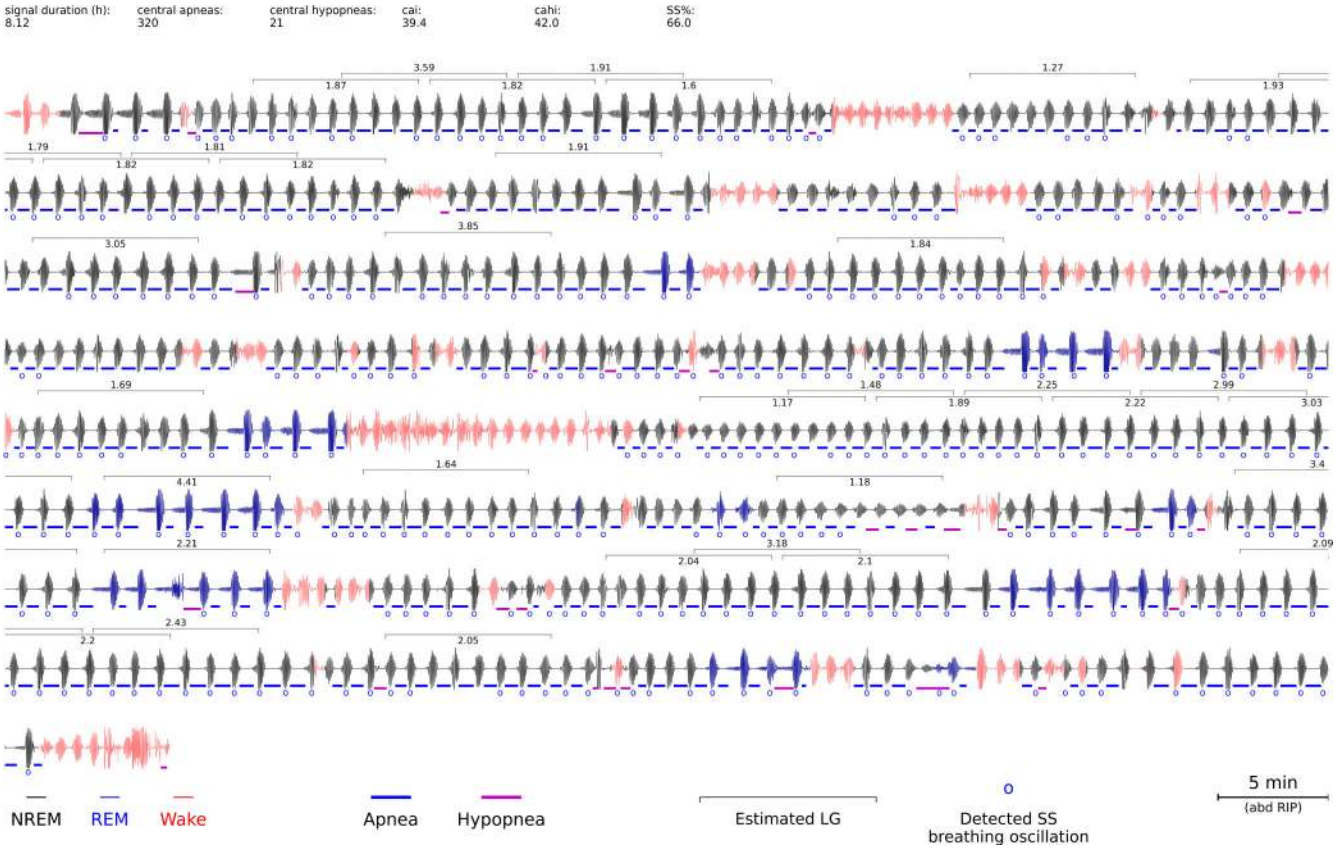

Figure 2:

Full-night example of patient showing periodic breathing, including estimations for the variable loop gain (LG) parameter for all 8-minute segments of consecutive rapid eye movement or non-rapid eye movement sleep. Note that the respiratory events and high self-similarity (SS) breathing oscillations are automatically labelled by our SS detector.

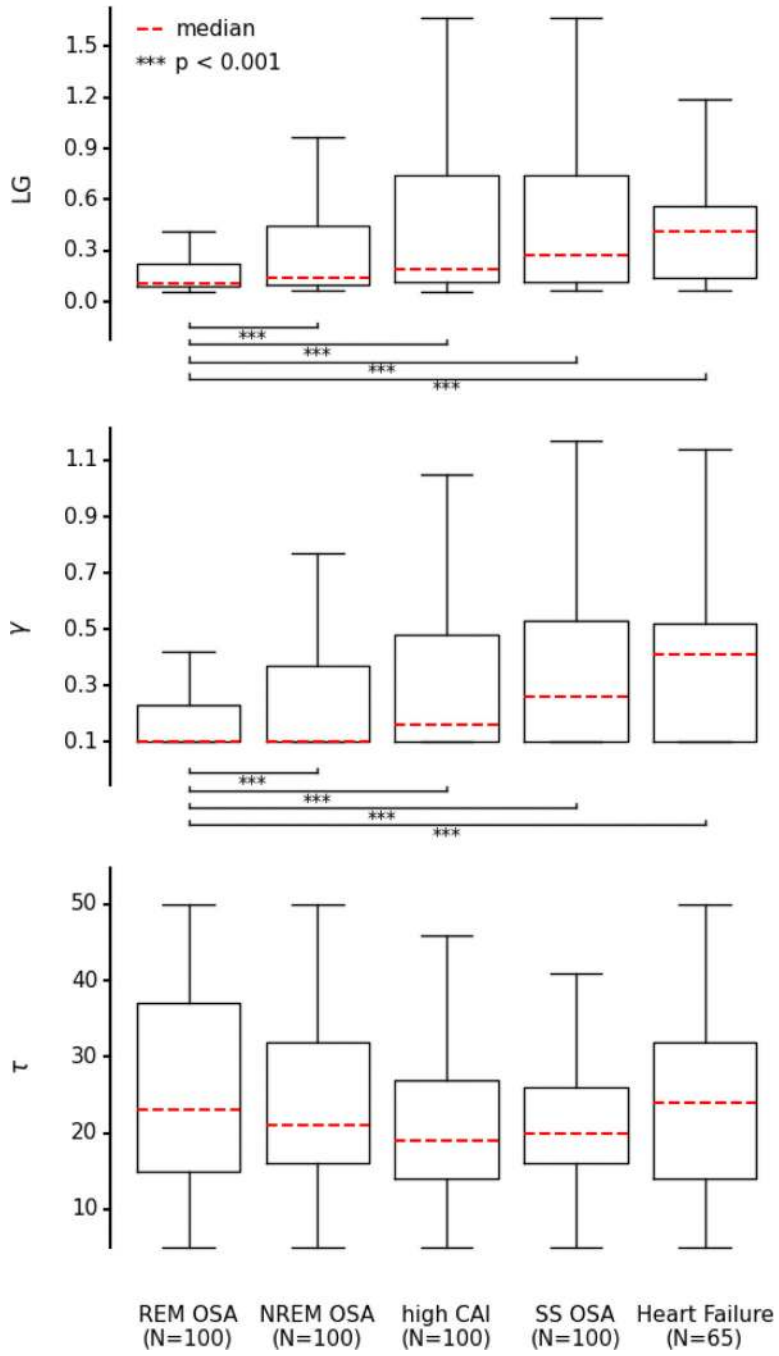

Figure 3:

Boxplots of the distribution of estimated loop gain (LG), controller gain (γ), and delay (τ) parameters across the different ventilatory control profile groups. Compared to the 'REM OSA' group all other groups showed a statistically significant increase in median LG/gain. The median τ was highest for the heart failure patients. OSA=obstructive sleep apnea, REM=rapid eye movement, NREM=non-REM, CAI=central apnea index, SS=self-similarity.

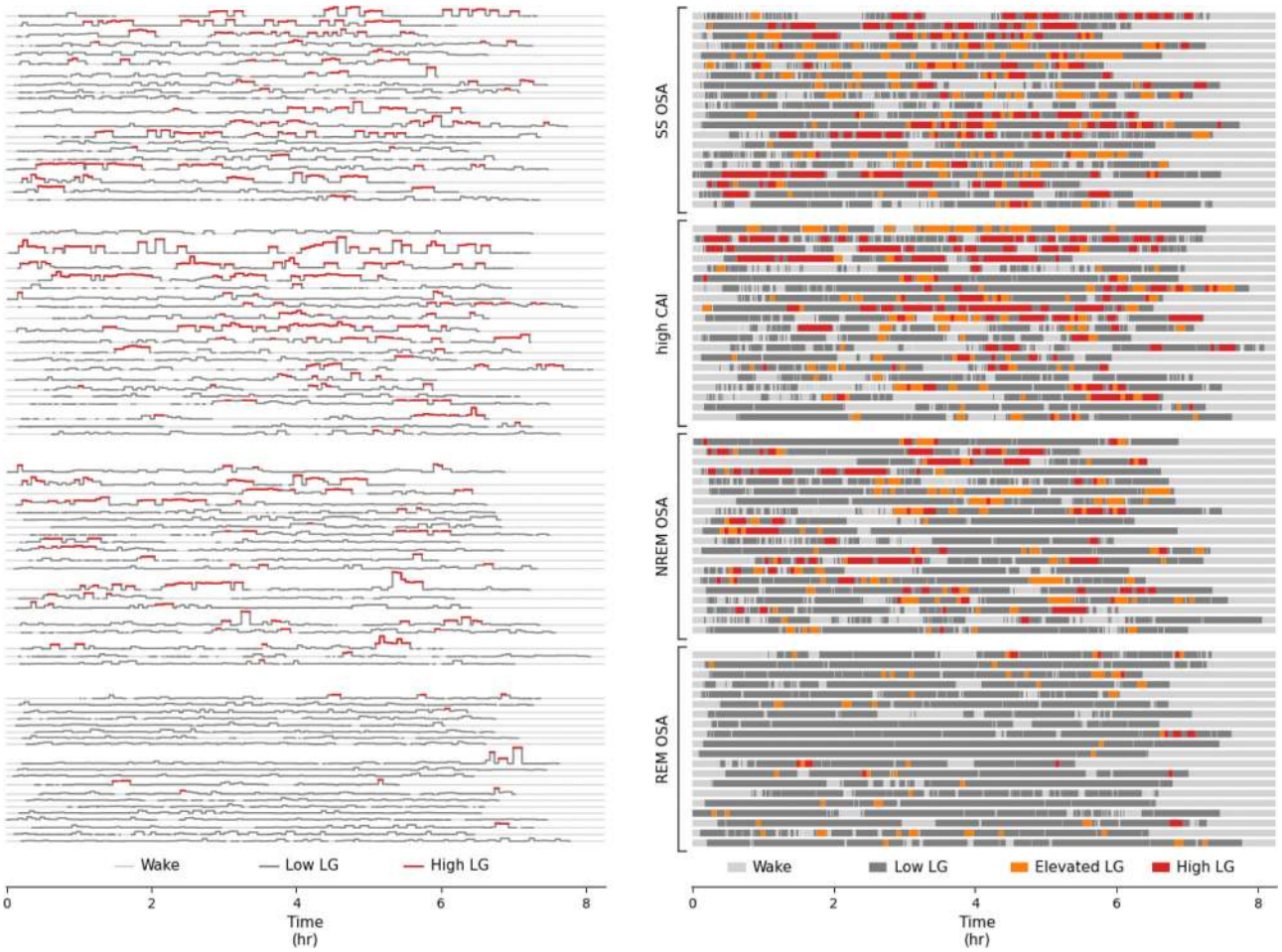

Figure 4:

Swimmer plots and bar graphs left and right respectively, of 20 individuals from the MGH ventilatory control profiles visualizing the proportion of elevated loop gain (LG) estimations across overnight recordings. OSA=obstructive sleep apnea, REM=rapid eye movement, NREM=non-REM, CAI=central apnea index, SS=self-similarity.

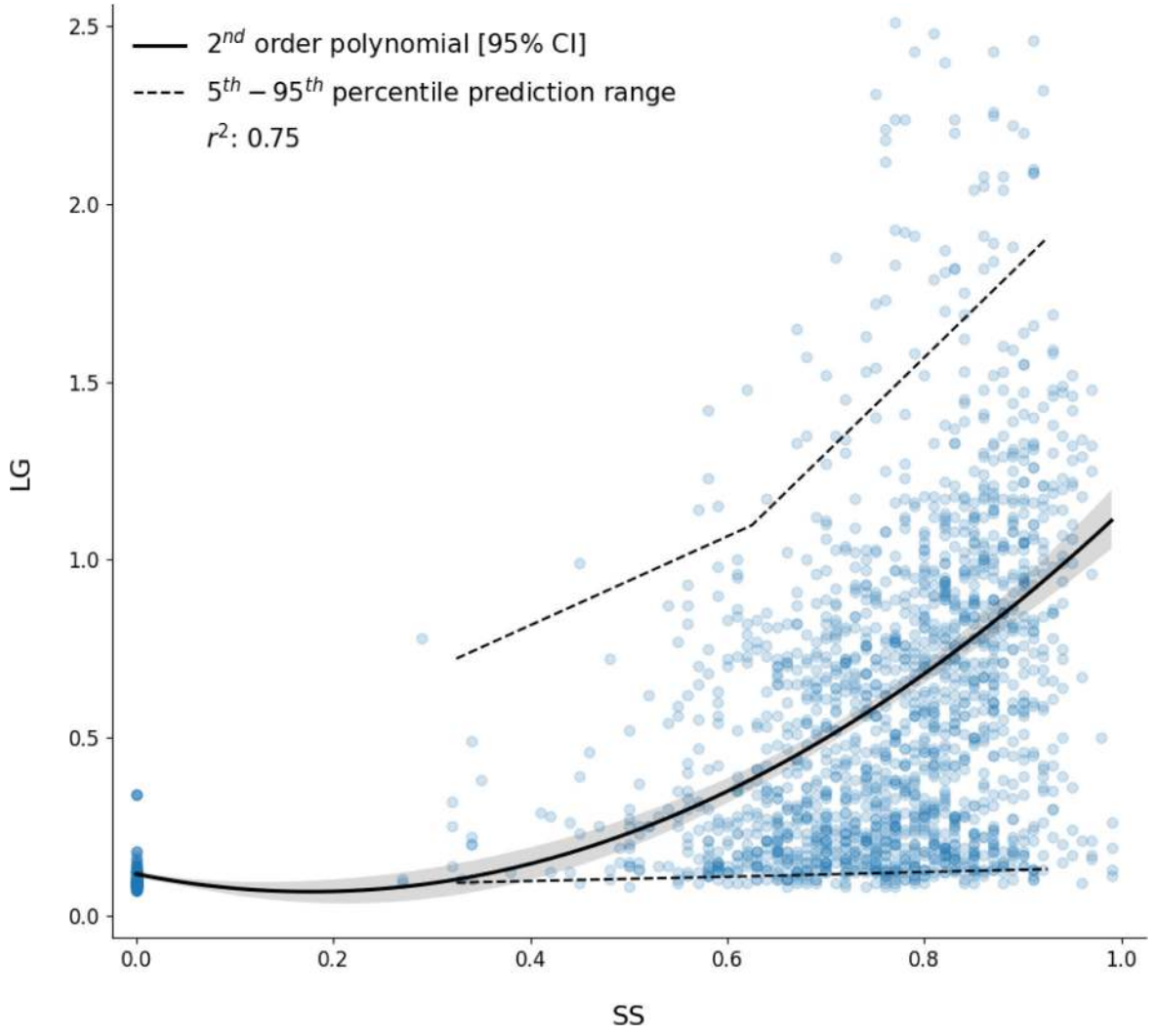

Figure 5:
Scatter plot showing the relationship between loop gain (LG) and self-similarity (SS), including the 5th-95th percentile range of all data points, from 100 patients. A 2nd order polynomial was fit to the data together with its 95% confidence interval (CI).

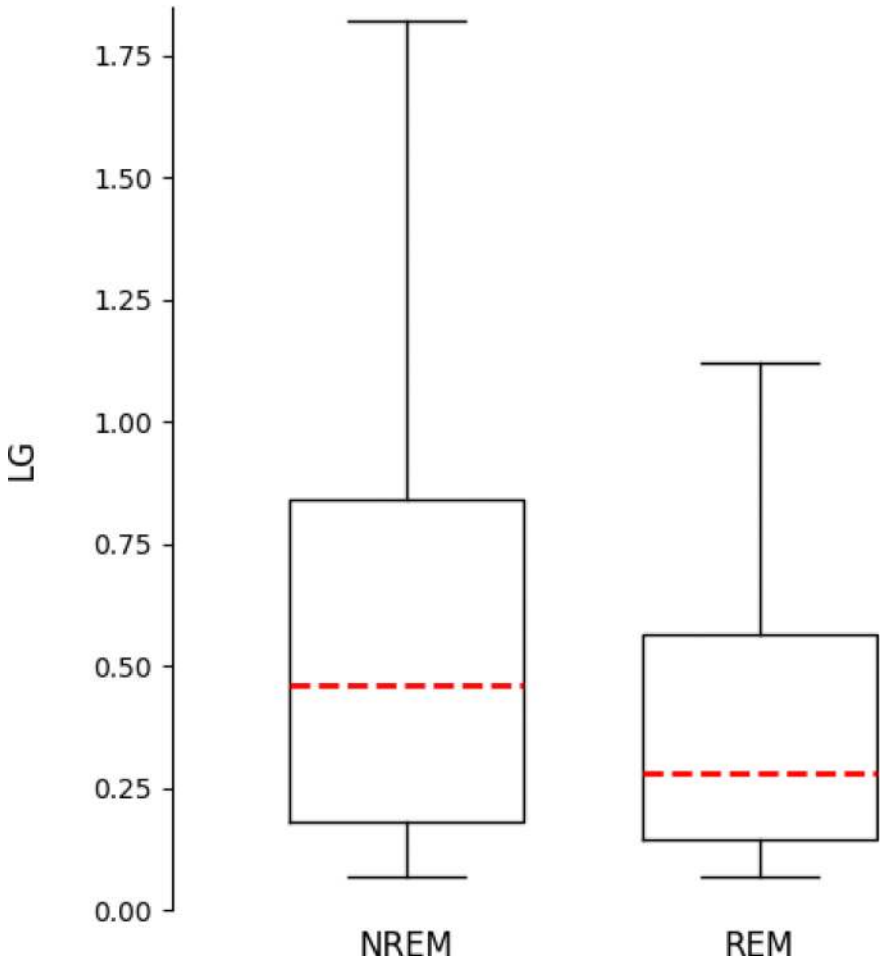

Figure 6:

Boxplots of the distribution of estimated loop gain (LG), during rapid eye movement (REM) and non-REM sleep segments from 100 patients with ranging levels of self-similarity (SS). The median LG across all NREM segments was notably higher compared to REM.

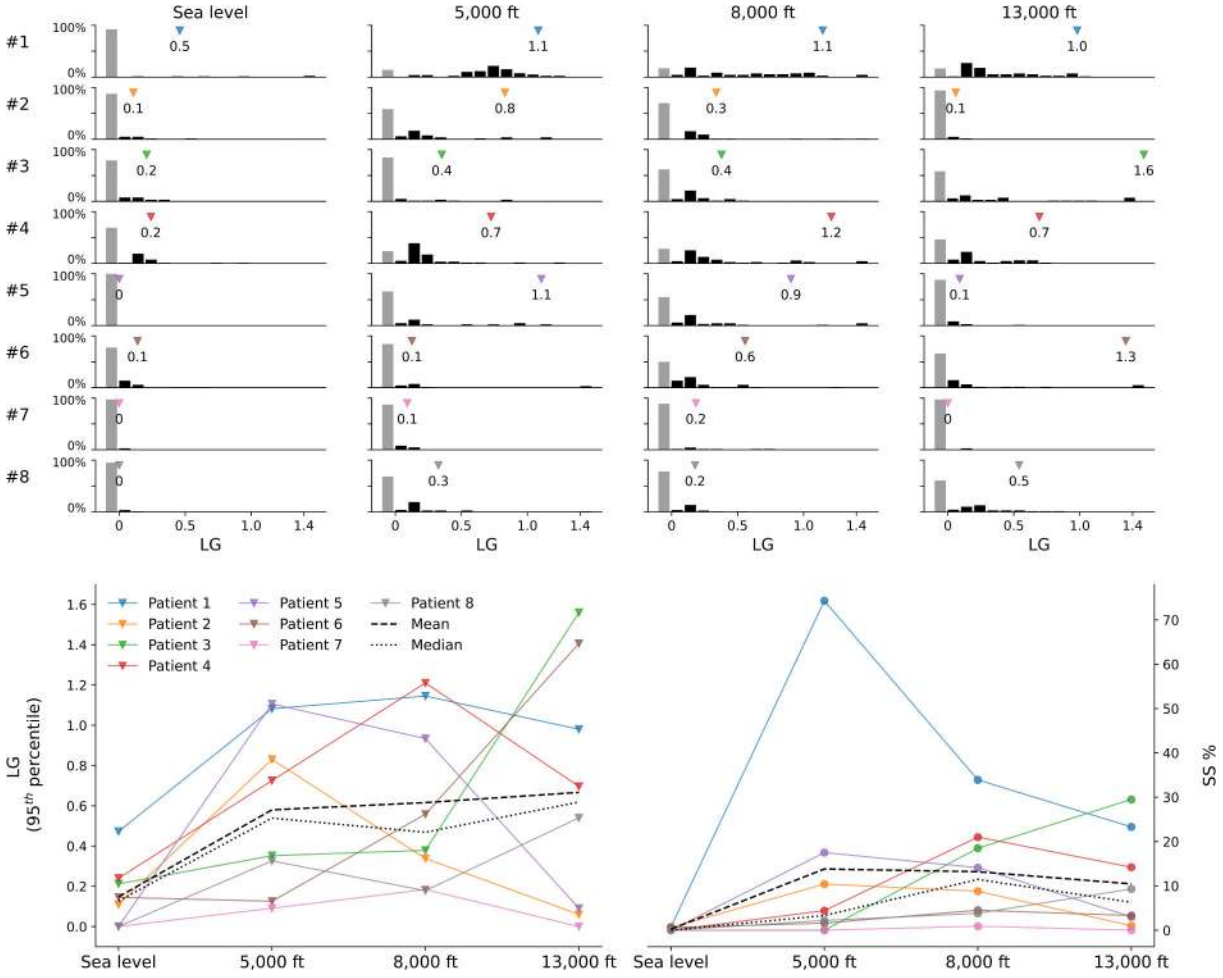

Figure 7:

Normalized histograms of the estimated loop gain (LG) distribution for 8 patients with each four recordings measured at increasing altitudes, i.e., participants spent one night each at sea level, 5000 feet, 9000 feet and then 13,000 feet for 2 weeks, as one continuous sequence. The bottom left spaghetti graph shows the trend of the 95th percentile estimated LG, as denoted by the triangles. The bottom right subfigure shows the automatically detected percentage of sleep with high SS breathing oscillations.

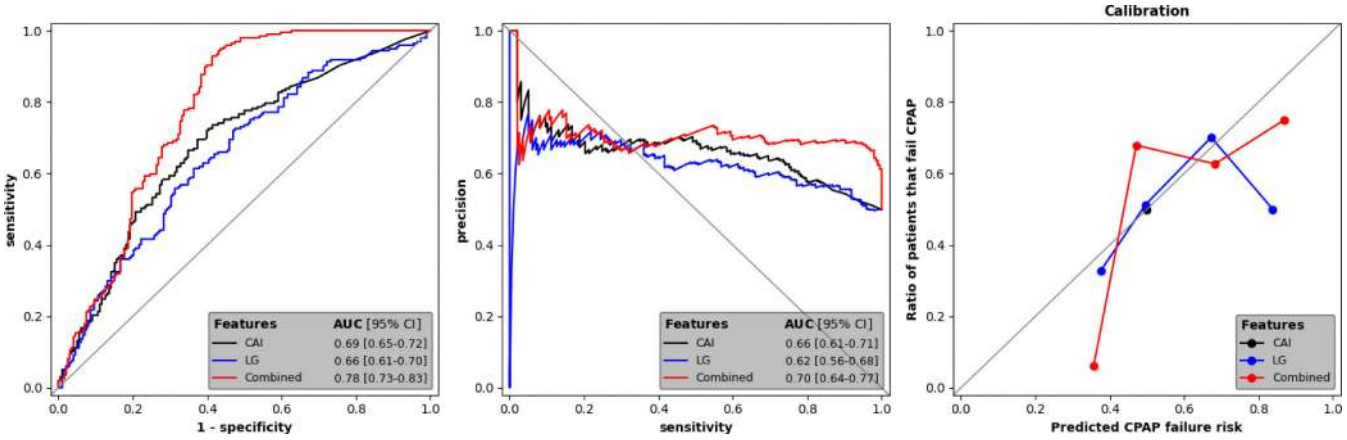

Figure 8:

Receiver Operating Characteristic (ROC), Precision-Recall (PR), and calibration curves for the estimated high loop gain (HLG), central apnea index (CAI), and their combination as predictors of CPAP failure (defined as apnea-hypopnea index ≥30 or CAI ≥10 despite CPAP). The ROC and PR curves include area under the curve (AUC) values with 95% confidence intervals (CI) provided in the legends, while the calibration curves assess the agreement between predicted and observed failure rates.

Table 1:

Cohort demographics (mean ± SD).

Category	Bins	REM OSA	NREM OSA	SS OSA	High CAI	Heart Failure	SS range	Altitude
N		100	100	100	100	65	100	8
Sex	Female	70	27	30	27	21	39	5
	Male	30	73	70	73	44	61	3
Age	<20	3	3	0	1	0	2	0
	20–40	21	20	7	12	7	14	8
	40–60	49	41	39	35	21	42	0
	60–80	26	33	52	43	32	38	0
	>80	1	3	2	9	8	4	0
Race	White	61	77	80	88	58	82	6
	Black	13	5	5	2	5	6	0
	Asian	3	3	3	3	0	2	0
	Other	18	9	5	4	0	8	2
	Unavailable	6	66	7	3	2	2	0
CAI		1.2 ±1.9	5.6 ±18.8	2.0 ±1.4	24.4 ±19.0	4.7 ±11.2	3.9 ±6.3	-
AHI (3%)	5–15	0	0	0	0	16	0	-
	15–30	80	30	3	1	23	33	-
	>30	20	70	97	99	26	67	-
AHI (4%)	5–15	0	0	6	0	30	28	-
	15–30	95	65	40	21	14	41	-
	>30	5	35	53	79	21	31	-
Medications	Info available for	58	51	50	61	-	50	-
	Hypertension	1	0	0	2	-	1	-
	Cardiac	3	1	0	0	-	0	-
	Sleep	4	4	0	4	-	3	-
	Antidepressants	3	2	0	1	-	1	-
	Antiseizure	0	0	0	1	-	0	-
	Opiates	4	0	1	2	-	1	-
	Benzodiazepines	1	2	2	2	-	1	-
	Diabetic	6	2	4	2	-	2	-
	Z-drugs	0	1	0	3	-	2	-
	Stimulants	3	3	0	2	-	1	-
	Neuroleptics	0	0	0	1	-	0	-
	RLS / PLMS	0	0	0	1	-	0	-
	Immune	1	0	1	1	-	1	-
	Neurodegenerative	0	1	0	0	-	0	-
	Other	39	40	31	48	-	30	-

OSA, obstructive sleep apnea. CAI, central apnea index. AHI, apnea hypopnea index. SS, self-similarity.